Dynamic generation of Debye diffraction-limited multifocal arrays for direct laser printing nanofabrication

Han Lin, Baohua Jia, and Min Gu*

Centre for Micro-Photonics and CUDOS, Faculty of Engineering and Industrial Sciences, Swinburne University of Technology, P. O. Box 218, Hawthorn, Victoria 3122, Australia
**Corresponding author: mgu@swin.edu.au*

Received October 18, 2010; revised December 20, 2010; accepted December 22, 2010; posted January 6, 2011 (Doc. ID 136653); published January 31, 2011

We propose a Debye-theory-based iterative method to produce accurate phase patterns for generating highly uniform diffraction-limited multifocal arrays with a high-NA objective. It is shown that by using the Debye method, the uniformity of the diffraction-limited focal arrays can reach 99%, owing to the critical consideration of the depolarization effect associated with high-NA objectives. The generated phase patterns are implemented in fast dynamic laser printing nanofabrication for the generation of individually controlled high-quality microvoid arrays in a solid polymer material by a single exposure of a femtosecond laser beam. As a result of the high-quality multifocal arrays, functional three-dimensional photonic crystals possessing multiple stopgaps with suppression up to 80% in transmission spectra are demonstrated.

OCIS codes: 220.4610, 090.1970.

Owing to its intrinsic advantage of high processing efficiency, the generation of multifocal spot arrays has gained increasing interest in various fields, including multiphoton multifocal microscopic imaging, optical trapping and manipulation, and laser micro/nano fabrication [1–11]. There are diverse ways to produce multifocal spot arrays, for example, using microlens arrays [1,6,7], diffractive optical elements [2,3,8], and spatial light modulators (SLMs) [4,5,9–11]. Among these approaches, using an SLM is the preferable method in most applications, owing to its capability to dynamically update the intensity distributions in the focal plane by varying the incident phase patterns.

Generating accurate phase patterns for highly uniform diffraction-limited multifocal arrays is vital for SLM-assisted applications for control of the light-matter interaction. Unfortunately, highly uniform diffraction-limited arrays have not been achieved, because of the inaccuracy of phase patterns arising from the use of conventional fast Fourier transform methods [12–15]. The key reason for this problem is that the depolarization effect in the focal region of a high-NA objective, which significantly alters the phase distribution [16–18], has been totally ignored. Under such a circumstance, conventional paraxial-approximation-based phase-retrieval methods [12–15] are no longer accurate enough to represent the actual focusing process of high-NA objectives for generating highly uniform diffraction-limited multifocal arrays.

In this Letter, we develop a phase-retrieval method based on the Debye theory for the generation of diffraction-limited multifocal arrays under high-NA focusing conditions. Through implementation of a controlling factor in the phase generation process, the intensity uniformity of a diffraction-limited multifocal array can be significantly improved, from 60% to 99% for high-NA objectives. Combined with a dynamic laser printing (DLP) nanofabrication system, this multifocal array facilitates the fast and dynamic fabrication of high-quality two-dimensional (2D) microvoid arrays with or without embedded arbitrary defects. Its high quality allows us to fabricate functional three-dimensional (3D) photonic crystals (PhCs) with scalable multi-order stopgaps, which present more than 80% suppression in transmission.

A high-NA objective DLP fabrication setup for multifocal array generation is shown in Fig. 1, in which two $4f$ systems are included for the experimental implementation. The goal of our Debye-theory-based phase-retrieval method is achievement of the diffraction-limited intensity distribution at the focal plane (FP) of the high-NA objective by controlling the phase at the back aperture plane (BAP). The key physical step is to use the Debye theory [16], rather than the Fourier transform, to calculate the intensity distributions I^{im} and phase information Φ^{im} in the focal region from the phase Φ^{BA} at the BAP. The Debye theory describes the depolarization effect of a high-NA objective by calculating the three orthogonal field components E_x, E_y, E_z, separately. This is significantly different from the paraxial approximation theory [16], which does not consider the vectorial nature. The overall intensity is the sum of the modular square of the three components, which is expressed as [16]

$$I = |E_x|^2 + |E_y|^2 + |E_z|^2. \tag{1}$$

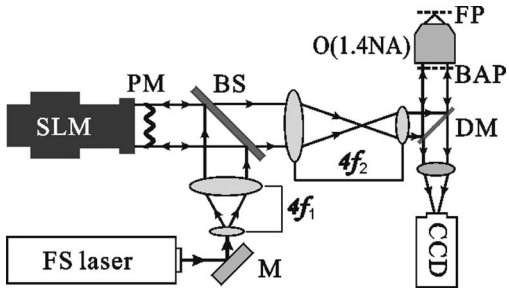

Fig. 1. Schematic of the experimental setup for the DLP nanofabrication system. M, mirror; PM, phase modulation; BS, beam splitter; DM, dichroic mirror; O, objective; FP, focal plane; BAP, back aperture plane.

To ensure that a Debye diffraction-limited multifocal array is achieved in the FP, we introduced a controlling factor M to correct the intensity of each individual focal spot. For the kth spot in the nth loop, the individual modification factor M_n^k is defined as

$$M_n^k = M_{n-1}^k \frac{I_{\text{im}}^k}{I_n^k}, \tag{2}$$

where I_{im}^k is the desired normalized intensity of the kth spot, I_n^k is the intensity of the kth focal spot normalized by the average intensity, and the overall controlling factor M is $M = \sum_{k=1}^{N} M_n^k$, where N is the number of the spots in the array. The modified desired field can be expressed as

$$\bar{E}^{\text{im}} = \sqrt{I^{\text{im}} M} \exp(i\Phi^{\text{im}}). \tag{3}$$

Thus Eq. (3) overcomes the stagnation problems in the conventional method [13] and leads to individual control of the amplitude of each focal spot. Once the geometrical location of an array is given, the use of Eqs. (1)–(3) results in accurate phase patterns for highly uniform diffraction-limited multifocal arrays through an iterative process.

To experimentally verify our method, we implemented the phase design into the DLP nanofanbrication system, as shown in Fig. 1. An 800 nm femtosecond (FS) laser beam is expended that illuminates an SLM (Holoeye Pluto) through the first $4f$ system ($4f_1$). Through the second $4f$ ($4f_2$) imaging system, the phase modulation (PM) from the SLM is transferred to the BAP of the high-NA objective (Olympus, UPLSAPO 100×, 1.40 NA). An array of diffraction-limited focal spots that is of the desired pattern can be generated at the FP of the objective. A CCD camera is used to view the fabrication process *in situ*.

An example of the generated phase pattern, which is composed of 1080×1080 (256 gray levels) pixels, for a 200-spot array is shown in Fig. 2(a). The uniformity of the array is defined as

$$u = 1 - \frac{I_{\max} - I_{\min}}{I_{\max} + I_{\min}}, \tag{4}$$

where the $I_{\max}$ and $I_{\min}$ are the maximum and minimum intensities of the foci in the array. The intensity distribution resulting from this phase pattern in the focal plane of the objective, calculated using the Debye theory, is shown in Fig. 2(b); uniformity of 99% is achieved. An enlarged focal spot from the array, highlighted in Fig. 2(c), is identical to the intensity distribution for a single focal spot calculated using the Debye theory [Fig. 2(d)]. As expected, the shape of the highlighted focal spot is elliptical owing to the depolarization effect. The FWHM of the focal spots in both the x and y directions in the whole array are found to be identical [Fig. 2(e)], which indicates that the diffraction-limited condition is achieved for each focal spot in the array.

To further demonstrate the high quality of the multifocal array achieved by our method, we compared the uniformity and the rms error of the array from the phase patterns generated using the Debye method and the conventional Gerchberg–Saxton (GS) method [12]. The

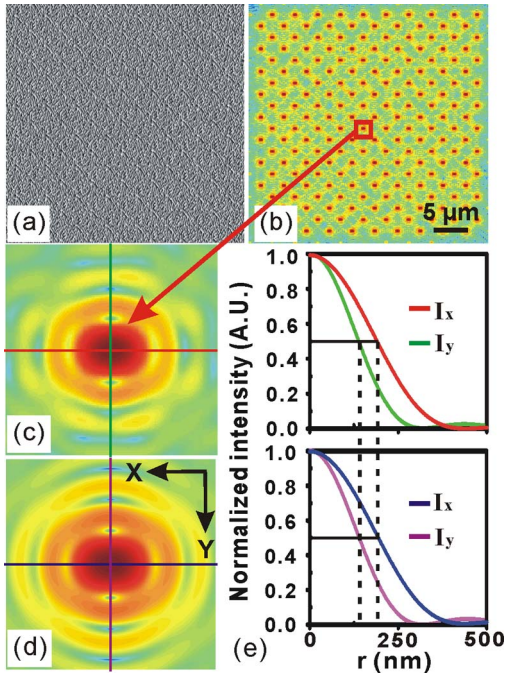

Fig. 2. (Color online) (a) Phase pattern consisting of 1080×1080 (256 gray levels) pixels for a 200-spot array; (b) calculated intensity distribution from the phase pattern using the Debye integral; (c) density plot for one focal spot in the array; (d) density plot for a single focal spot; (e) intensity cross sections along the marked color lines of the spots. The scale bar is 5 μm.

uniformity versus the number of iterations is shown in Fig. 3(a). The uniformity and the rms error of a 200-focal spot array for the GS method are approximately 62% and 0.15, respectively. The uniformity cannot be further improved by increasing the number of iterations due to the inaccurate transform process and the stagnation problems [13]. In contrast, the Debye method can achieve uniformity of up to 95% and rms error down to 0.01 within the first several tens of iterations. Within 200 iterations, Debye method can reach uniformity over 99% and rms error down to 0.001, respectively. These calculated results were experimentally verified.

The phase pattern in Fig. 2(a) was used to generate an array of voids in a solid polymer material (NOA 63, Norland Products Inc., Cranbury, NJ, USA) [19], based on the multiphoton-induced microexplosion mechanism [20]. The resultant void array by a single exposure of 10 ms at the power of 4 mW is shown in Fig. 3(b). It was found that the ratio of the incoming beam to the objective aperture could not be less than 0.95, at which the distortion due to the chromatic aberration was still negligible, so that uniformity of over 90% in a circular region of 80 μm in diameter could be obtained. Controllable defects, which are of great importance in functional photonic devices, can also be achieved by individually controlling the intensity of each focal spot. This is possible only with a highly uniform spot array, because otherwise the designed defects tended to be overwhelmed by the undesired fluctuation induced by the nonuniformity. The focal spot arrays with designed Y junction defects are shown in Figs. 3(c) and 3(d), in which defects are produced by removing or enhancing some of the spots in the array.

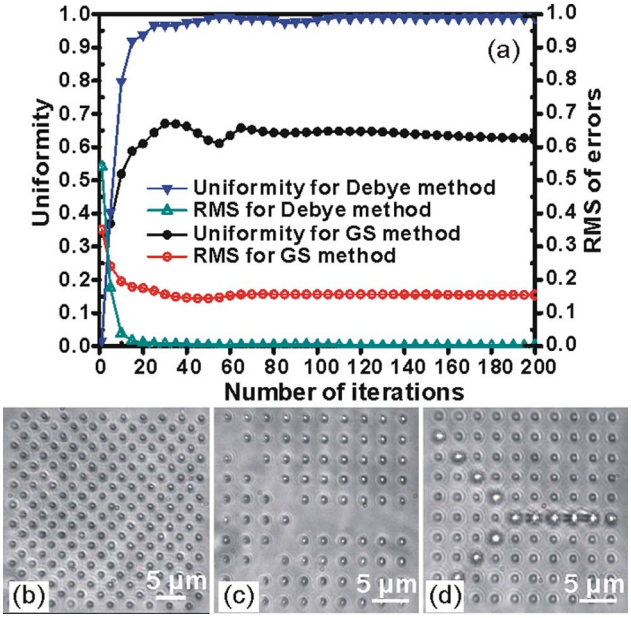

Fig. 3. (Color online) (a) Dependence of uniformity and rms error on the number of iterations calculated using the Debye method and the GS algorithm; (b) transmission optical microscopic image of a fabricated 200-void array (Media 1); (c) a 100-void array with a Y-shaped defect fabricated by removing some of the focal spots; (d) a 100-void array with a Y-shaped defect fabricated by enhancing the exposure intensity of some of the focal spots. Scale bar, $5\,\mu$m.

The high-quality 2D void arrays [Fig. 3(b)] can be stacked into a 3D PhC. A 40-layer 3D PhC with a face-centered-cubic (FCC) lattice can be fabricated layer by layer instead of spot by spot, using the DLP setup shown in Fig. 1. The entire PhC was fabricated with 40 exposures in 40 s, which is more than 2 orders of magnitude faster than conventional direct laser writing fabrication of the same structure (1 h) [20]. Figures 4(a) and 4(b) show the transmission spectra measured using a Fourier transform IR [20] spectrometer of two FCC PhCs stacked in the [100] direction with lattice constants of 3.5 and $4\,\mu$m, respectively. Not only first-order stopgaps, but also higher-order stopgaps are observed. The average suppression ratios of the transmission of the first- and second-order stopgaps are approximately 80% and 25%, respectively. The center wavelength dependence of the first- and second-order stopgaps on the lattice constant are plotted in Fig. 4(c), where a linear relationship can be observed, as expected.

In summary, based on the Debye theory, we have developed a method for the accurate phase pattern generation of highly uniform diffraction-limited multifocal arrays for high-NA objectives. The proposed method is able to accurately represent the physical depolarization process of high-NA focusing. The application of the method in nanofabrication has allowed us to perform fast and dynamic parallel layer printing of 2D arrays of high-quality voids with controlled defects, as well as 3D PhCs with multi-order stopgaps. The technique opens the possibility for other multifocal-related applications, including multifocal microscopy and optical tweezers.

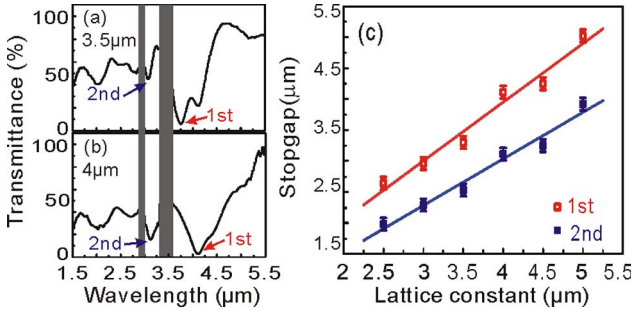

Fig. 4. (Color online) Transmission spectra of 3D FCC void PhCs with lattice constants (a) $3.5\,\mu$m and (b) $4\,\mu$m. The gray areas are the absorption bands of the material. The dependence of the stopgap positions on the lattice constant is shown in (c).

This work is produced with the assistance of the Australian Research Council (ARC) under the Centres of Excellence Program. CUDOS is an ARC Centre of Excellence. Baohua Jia is supported by ARC Australian Postdoctoral Fellowship (APD) grant DP0987006. The authors acknowledge helpful discussion with Guangyong Zhou and technical support from Benjamin P. Cumming.

References

1. J. Kato, N. Takeyasu, Y. Adachi, H. B. Sun, and S. Kawata, Appl. Phys. Lett. **86**, 044102 (2005).
2. G. Lee, S. H. Song, C. H. Oh, and P. S. Kim, Opt. Lett. **29**, 2539 (2004).
3. M. Yamaji, H. Kawashima, J. Suzuki, and S. Tanaka, Appl. Phys. Lett. **93**, 041116 (2008).
4. N. J. Jenness, K. D. Wulff, M. S. Johannes, M. J. Padgett, D. G. Cole, and R. L. Clark, Opt. Express **16**, 15942 (2008).
5. Z. Kuang, D. Liu, W. Perrie, S. Edwardson, M. Sharp, E. Fearon, G. Dearden, and K. Watkins, Appl. Surf. Sci. **255**, 6582 (2009).
6. J. Bewersdorf, R. Pick, and S. W. Hell, Opt. Lett. **23**, 655 (1998).
7. A. H. Buist, M. Muller, J. Squier, and G. J. Brakenhoff, J. Microsc. **192**, 217 (1998).
8. L. Sacconi, E. Froner, R. Antolini, M. R. Taghizadeh, A. Choudhury, and F. S. Pavone, Opt. Lett. **28**, 1918 (2003).
9. J. E. Curtis, B. A. Koss, and D. G. Grier, Opt. Commun. **207**, 169 (2002).
10. R. L. Eriksen, V. R. Daria, and J. Glückstad, Opt. Express **10**, 597 (2002).
11. Y. Roichman and D. G. Grier, Opt. Lett. **31**, 1675 (2006).
12. R. W. Gerchberg and W. O. Saxton, Optik (Jena) **35**, 237 (1972).
13. J. R. Fienup and C. C. Wackerman, J. Opt. Soc. Am. A **3**, 1897 (1986).
14. J. Miao, D. Sayre, and H. N. Chapman, J. Opt. Soc. Am. A **15**, 1662 (1998).
15. S. G. Podorov, K. M. Pavlov, and D. M. Paganin, Opt. Express **15**, 9954 (2007).
16. M. Gu, *Advanced Optical Imaging Theory* (Springer, 1999).
17. J. W. M. Chon, X. Gan, and M. Gu, Appl. Phys. Lett. **81**, 1576 (2002).
18. B. Jia, X. Gan, and M. Gu, Appl. Phys. Lett. **86**, 131110 (2005).
19. M. J. Ventura, M. Straub, and M. Gu, Appl. Phys. Lett. **82**, 1649 (2003).
20. G. Zhou, M. J. Ventura, M. Vanner, and M. Gu, Opt. Lett. **29**, 2240 (2004).